

## Supplementary information

**Engineering heterostructured Mo<sub>2</sub>C/MoS<sub>2</sub> catalyst with hydrophilicity/aerophobicity via carbothermal shock for efficient alkaline hydrogen evolution**

Hao Xiong, Xinren Zhang, Xu Peng, Dengke Liu, Yimeng Han and Fei Xu\*

State Key Laboratory of Solidification Processing, Center for Nano Energy Materials, School of Materials Science and Engineering, Northwestern Polytechnical University, Xi'an 710072, P. R. China.

E-mail: feixu@nwpu.edu.cn (F. Xu)

## Materials and Methods

### 1. Materials

All the reagents were purchased from Sigma-Aldrich and utilized as received without any further purification, including molybdenum disulfide ( $\text{MoS}_2$ ), ammonium molybdate tetrahydrate ( $(\text{NH}_4)_6\text{Mo}_7\text{O}_{24}\cdot 4\text{H}_2\text{O}$ ), glucose ( $\text{C}_6\text{H}_{12}\text{O}_6$ ), potassium hydroxide (KOH), ethanol absolute, isopropanol, Pt/C (20 wt.% Pt on activated carbon) and Nafion (5.0 wt.%). Carbon paper (CP) was purchased from SCl Materials Hub. All aqueous solutions were prepared with deionized (DI) water (resistivity:  $18.2 \text{ M}\Omega \text{ cm}^{-2}$ ) from a Millipore deionized water system.

### 2. Preparation of $\text{Mo}_2\text{C}/\text{MoS}_2\text{-CP}$

$\text{MoS}_2$  with a fixed mass of 64 mg as well as  $(\text{NH}_4)_6\text{Mo}_7\text{O}_{24}\cdot 4\text{H}_2\text{O}$  and  $\text{C}_6\text{H}_{12}\text{O}_6$  were firstly weighed, which were sequentially added into 20 mL of deionized water and ultrasonicated for 30 min to mix well. To explore the optimal precursor ratio, samples with different molar ratios (1/3, 2/3, 1, 1.5, 3, and 6) of  $(\text{NH}_4)_6\text{Mo}_7\text{O}_{24}\cdot 4\text{H}_2\text{O}$  and  $\text{MoS}_2$  were studied, where  $(\text{NH}_4)_6\text{Mo}_7\text{O}_{24}\cdot 4\text{H}_2\text{O}$  and  $\text{C}_6\text{H}_{12}\text{O}_6$  were of equal molar. The carbon paper (1 cm $\times$ 2 cm) was immersed in the above mixture solution, sonicated for 30 min, and then dried overnight at 60 °C in the oven. Accordingly, carbon paper uniformly loaded with precursors (S-CP) was put into a Joule heating system (temperature detection range: 700 °C-3000 °C). Setting the heating parameters as 24 A and 17 V, the materials were heated at 1500 °C under Ar atmosphere for 2 s, 20 s, and 60 s, respectively, to obtain the carbon paper loaded with Mo-based catalysts, denoted as  $\text{Mo}_2\text{C}/\text{MoS}_2\text{-CP}$ . The mass loading of the  $\text{Mo}_2\text{C}/\text{MoS}_2\text{-CP}$  with a molar ratio of 3:1 was about 1.1 mg  $\text{cm}^{-2}$ . Impressively, the carbothermal shock process was so fast that the heating and cooling process took no more than 2 seconds.

### 3. Preparation of $\text{Mo}_2\text{C-CP}$ and $\text{MoS}_2\text{-CP}$

$\text{Mo}_2\text{C-CP}$  was prepared similarly to  $\text{Mo}_2\text{C}/\text{MoS}_2\text{-CP}$  except that  $\text{MoS}_2$  was not added to the precursor solution.  $\text{MoS}_2\text{-CP}$  was prepared by the same method as  $\text{Mo}_2\text{C}/\text{MoS}_2\text{-CP}$ , without adding  $(\text{NH}_4)_6\text{Mo}_7\text{O}_{24}\cdot 4\text{H}_2\text{O}$  and  $\text{C}_6\text{H}_{12}\text{O}_6$  to the precursor solution.

#### **4. Preparation of Pt/C-CP**

The preparations of the Pt/C catalyst adopt the drip-cast procedure. 20 wt.% Pt/C (10 mg) and Nafion (50  $\mu\text{L}$ ) were dispersed in IPA (950  $\mu\text{L}$ ) with ultrasonication in ice water for 1 h. Then the dispersion (100  $\mu\text{L}$ ) was dripped onto the surface of carbon paper and dried overnight to obtain the Pt/C-CP.

#### **5. Characterization**

The scanning electron microscope (SEM, Nova NanoSEM450, FEI) and transmission electron microscope (TEM, Talos F200X, FEI) were utilized to characterize the morphology and nanostructure of the catalysts. With the assistance of ultrasonication, the samples were peeled from the carbon paper and dispersed on the copper mesh for TEM characterization. The X-ray photoelectron spectroscopy (Thermo Scientific K-Alpha X) was used for analyzing the chemical states of different elements. The crystal structure of different catalysts was explored via the X-ray diffractometer (MAXima\_X XRD-7000) with Cu  $K\alpha$  radiation. Contact angles between catalysts and electrolytes were investigated through the optical contact angle meter (KRÜSS DSA100). Hydrogen bubbles on the catalyst surface were photographed with an optical microscope (DEEP-OPTICALM3-B-C).

#### **6. Electrochemical Measurements**

We used a three-electrode system, in which the prepared electrodes were used as the working electrode, graphite rod as the counter electrode, and standard Hg/HgO as the reference electrode, to perform HER performance tests on an electrochemical workstation (CHI 660E, China). Linear sweep voltammetry (LSV) curves of HER were obtained by scanning at 5  $\text{mV s}^{-1}$  with 95%  $iR$  compensation in 1 M KOH. The Tafel slope ( $b$ ) was estimated by linearly fitting the curves of overpotential ( $\eta$ ) vs.  $\log |j|$  ( $j$ , current density) with the equation ( $\eta = b \log |j| + a$ ). To determine the electrochemical double-layer capacitance ( $C_{dl}$ ) values, CV curve measurements were carried out in the range of 0.3-0.4 V vs. the reversible hydrogen electrode at scanning rates of 20, 40, 60,

80, 100, and 120 mV s<sup>-1</sup>, respectively. The electrochemical active surface area (ECSA) can be calculated according to the following equation:  $ECSA = C_{dl}/C_s$ , where  $C_s$  is the specific capacitance and generally regarded as the same as the CP substrate (0.25 mF cm<sup>-2</sup>). Electrochemical impedance spectra (EIS) measurements were performed with a frequency range of 0.1 Hz to 1 MHz and an amplitude voltage of 10 mV. The HER stability of the Mo<sub>2</sub>C/MoS<sub>2</sub>-CP catalyst was evaluated by the chronoamperometry (CP) method performed at the current density of 10 mA cm<sup>-2</sup> using a multichannel electrochemical workstation (Bio-Logic SAS).

## Figures and Tables

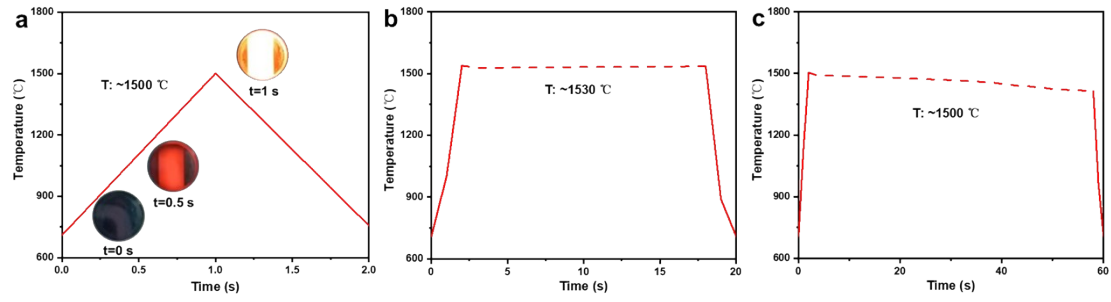


**Fig. S1** Temperature-Time curves of (a) 2 s, (b) 20 s and (c) 60 s for the synthesis of Mo<sub>2</sub>C/MoS<sub>2</sub>-CP.

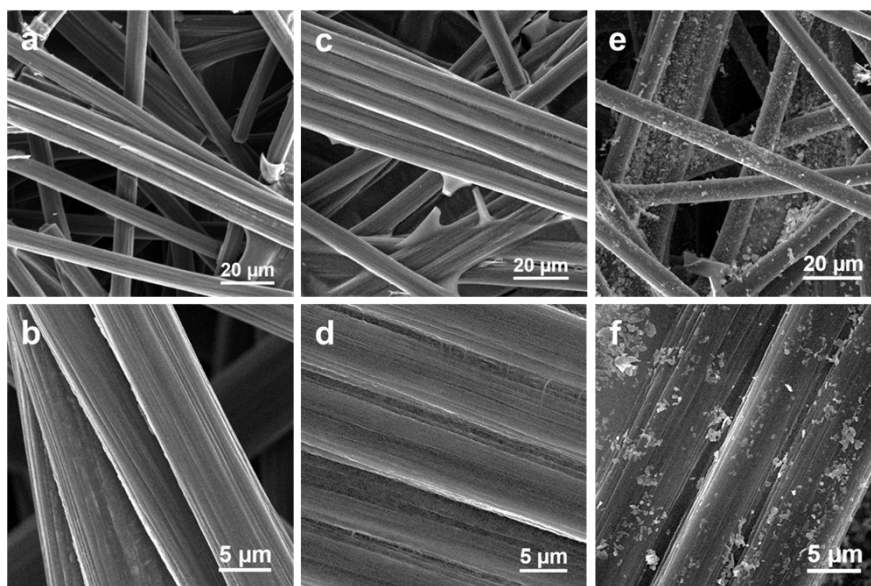


**Fig. S2** SEM images of (a, b) CP, (c, d) Mo<sub>2</sub>C-CP, and (e, f) MoS<sub>2</sub>-CP.

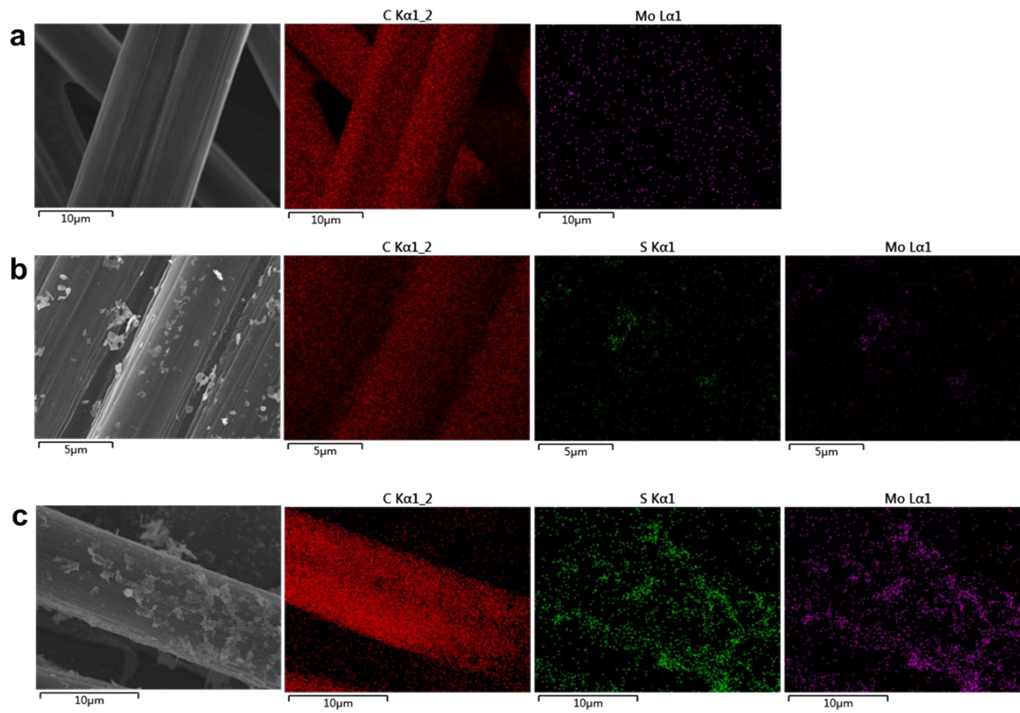


**Fig. S3** Elements mapping of (a) Mo<sub>2</sub>C-CP, (b) MoS<sub>2</sub>-CP, and (c) Mo<sub>2</sub>C/MoS<sub>2</sub>-CP.

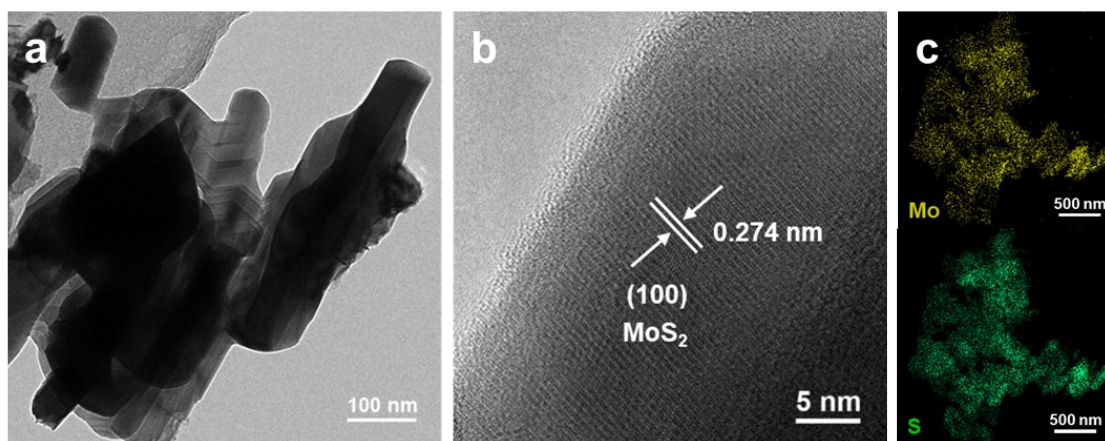


**Fig. S4** (a) TEM and (b) HRTEM images of MoS<sub>2</sub> in MoS<sub>2</sub>-CP; (c) elemental mappings of Mo and S.



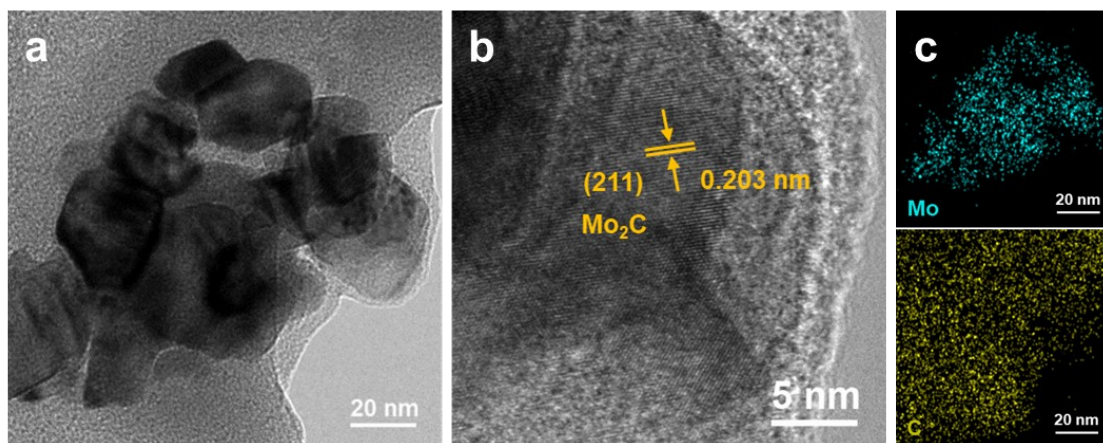


**Fig. S5** (a) TEM and (b) HRTEM images of Mo<sub>2</sub>C in Mo<sub>2</sub>C-CP; (c) elemental mappings of Mo and C.

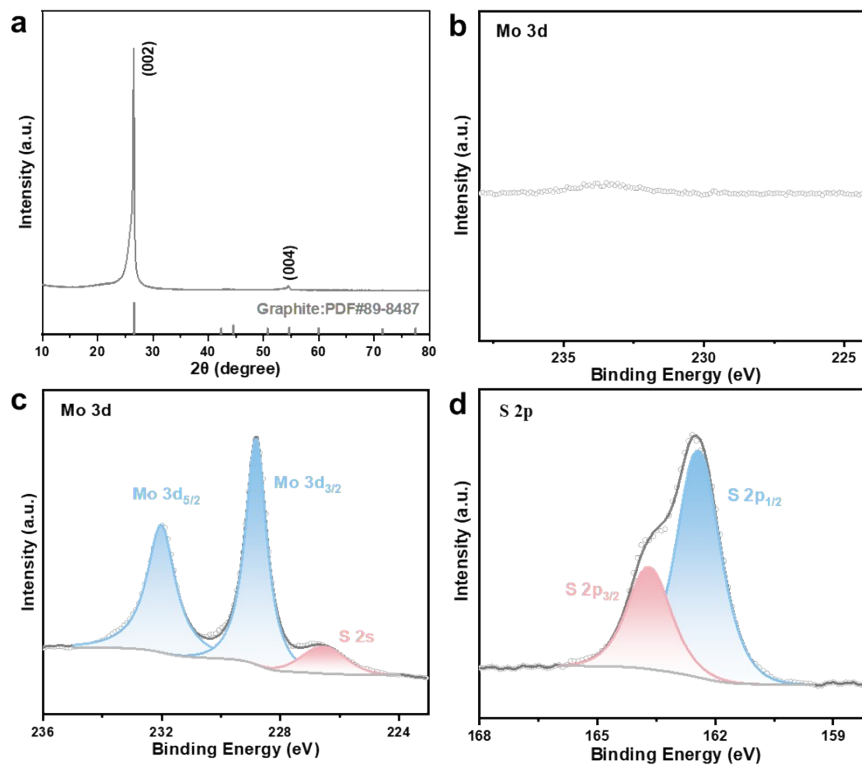


**Fig. S6** (a) XRD pattern of CP; XPS spectra of (b) Mo 3d in CP, (c) Mo 3d, and (d) S 2p in MoS<sub>2</sub>-CP.

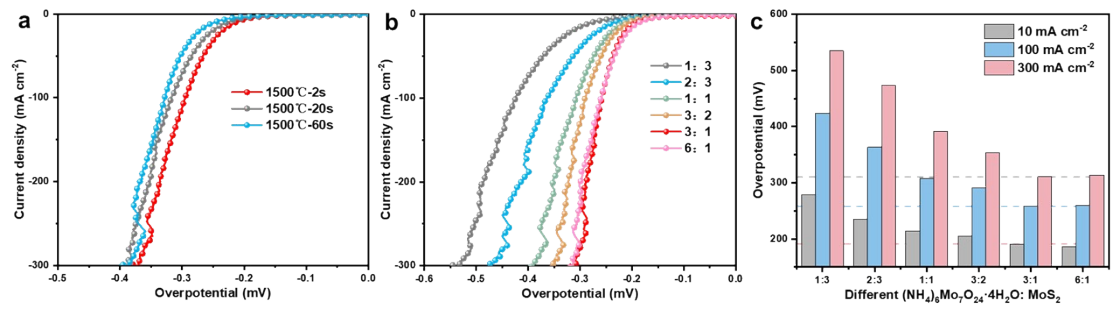


**Fig. S7** (a) LSV curves of Mo<sub>2</sub>C/MoS<sub>2</sub>-CP under different heating times; (b) LSV curves of Mo<sub>2</sub>C/MoS<sub>2</sub>-CP with different precursor ratios; (c) overpotential of Mo<sub>2</sub>C/MoS<sub>2</sub>-CP with different precursor ratios at 10, 100, and 300 mA cm<sup>-2</sup>, respectively.

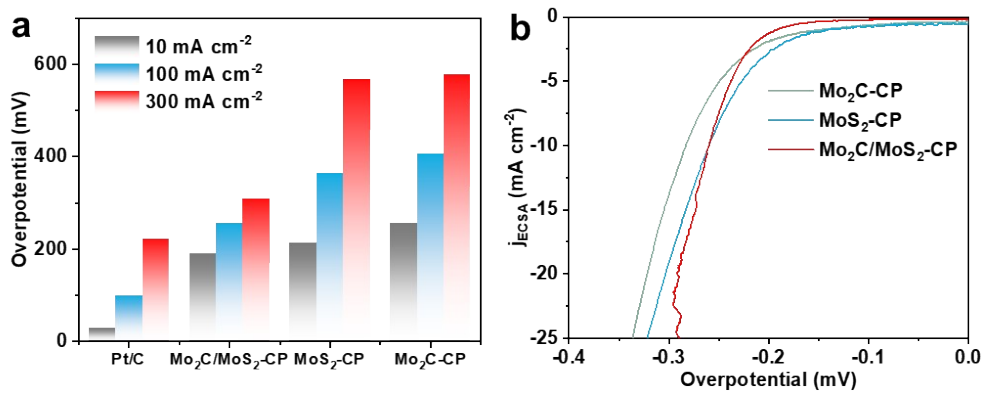


**Fig. S8** (a) Overpotential under different current densities; (b) LSV curves normalized by ECSA.

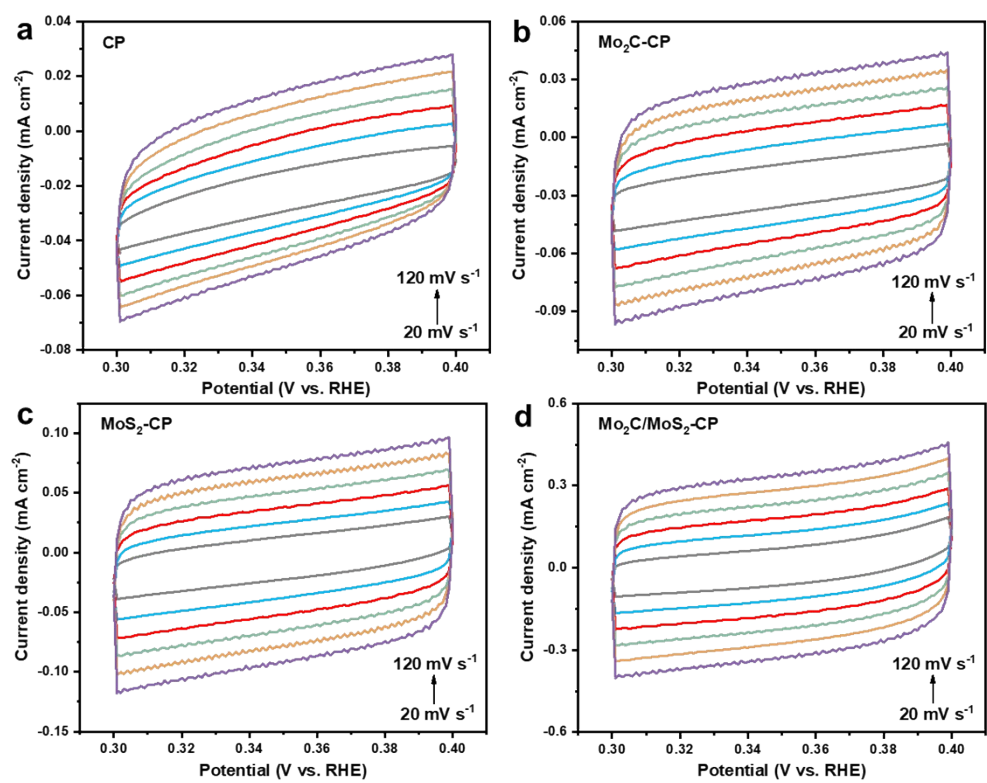


**Fig. S9** CV curves under different scan rates of (a) CP, (b) Mo<sub>2</sub>C-CP, (c) MoS<sub>2</sub>-CP, and (d) Mo<sub>2</sub>C/MoS<sub>2</sub>-CP.

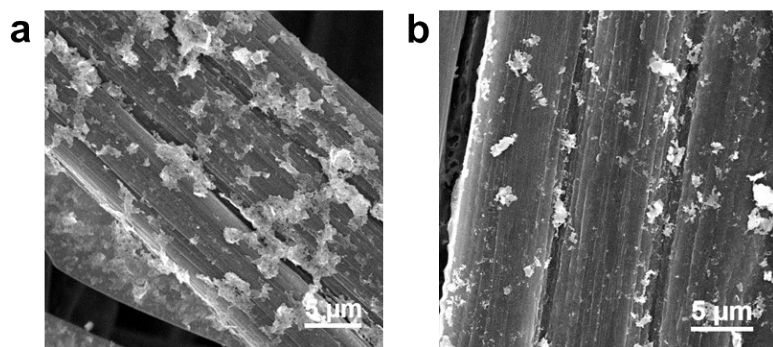


**Fig. S10** SEM images of Mo<sub>2</sub>C/MoS<sub>2</sub>-CP (a) before and (b) after the chronoamperometry test.

**Table S1.** Overpotential of Mo<sub>2</sub>C/MoS<sub>2</sub>-CP catalysts with different molar ratios of (NH<sub>4</sub>)<sub>6</sub>Mo<sub>7</sub>O<sub>24</sub>·4H<sub>2</sub>O: MoS<sub>2</sub> at 10, 100, and 300 mA cm<sup>-2</sup> in 1 M KOH.

<b>Molar ratio</b>	<b>Overpotential (mV)</b>		
	10 (mA cm <sup>-2</sup> )	100 (mA cm <sup>-2</sup> )	300 (mA cm <sup>-2</sup> )
1:3	278.5	423.9	535
2:3	235.6	363.1	473.6
1:1	214.5	307.7	391
3:2	205.6	290.8	353.1
3:1	190.8	258.4	310.8
6:1	186.5	259.9	313.9

**Table S2.** Overpotential of Pt/C, Mo<sub>2</sub>C-CP, MoS<sub>2</sub>-CP, and Mo<sub>2</sub>C/MoS<sub>2</sub>-CP catalysts at 10, 100, and 300 mA cm<sup>-2</sup> in 1 M KOH.

Sample	Overpotential (mV)		
	10 (mA cm <sup>-2</sup> )	100 (mA cm <sup>-2</sup> )	300 (mA cm <sup>-2</sup> )
Pt/C	30.4	100.4	223.6
Mo <sub>2</sub> C/MoS <sub>2</sub> -CP	190.8	258.4	310.8
MoS <sub>2</sub> -CP	214.4	365.9	568.1
Mo <sub>2</sub> C-CP	257.5	408.3	579.4



**Table S3.** The comparison of the catalytic performance of this Mo<sub>2</sub>C/MoS<sub>2</sub>-CP with previously reported MoS<sub>2</sub>-based electrocatalysts in 1 M KOH.

<b>Samples</b>	<b>Overpotential at 10 mV cm<sup>-2</sup> (mV)</b>	<b>Tafel slope (mV dec<sup>-1</sup>)</b>	<b>References</b>
Mo <sub>2</sub> C/MoS <sub>2</sub> -CP	191	64.5	This work
NiS <sub>2</sub> /MoS <sub>2</sub>	204	65	ACS Catal., 2017, 7, 6179-6187.
laser-treated MoS <sub>2</sub>	217	74.5	J. Alloy. Compd., 2020, 834, 155217.
Ni(OH) <sub>2</sub> /MoS <sub>2</sub>	227	105	Nanoscale, 2018, 10, 19074-19081.
1T/2H MoS <sub>2</sub>	236	46	J. Mater. Chem. A, 2017, 5, 2681-2688.
Co-BDC/MoS <sub>2</sub>	248	86	Small, 2019, 15, 1805511.
1T-2H MoS <sub>2</sub>	290	65	Adv. Energy Mater., 2018, 8, 1801345.

**Table S4.** Calculated electrochemical double-layer capacitance ( $C_{dl}$ ) and ECSA for selected as-prepared materials.

<b>Catalysts</b>	<b><math>C_{dl}</math> (mF cm<sup>-2</sup>)</b>	<b>ECSA</b>
CP	0.25	1
Mo <sub>2</sub> C-CP	0.42	1.68
MoS <sub>2</sub> -CP	0.66	2.64
Mo <sub>2</sub> C/MoS <sub>2</sub> -CP	2.16	8.64

**Table S5.** Fitting Impedance parameters for the equivalent circuit of CP, Mo<sub>2</sub>C-CP, MoS<sub>2</sub>-CP, and Mo<sub>2</sub>C/MoS<sub>2</sub>-CP catalysts.

<b>Catalysts</b>	$R_s/\Omega$	$R_{ct}/\Omega$	CPE-P	CPE-T
CP	1.1	132.2	0.946	0.00010
Mo <sub>2</sub> C-CP	1.2	16.1	0.934	0.00026
MoS <sub>2</sub> -CP	1.2	10.0	0.915	0.00064
Mo <sub>2</sub> C/MoS <sub>2</sub> -CP	1.2	1.2	0.901	0.00225